Spring 2019

The Impacts of Episodic Floods, Droughts, Turbidites on Organic Carbon Burial over the past 2,000 Years in the Santa Barbara Basin, California

Caitlyn Sarno

THE IMPACTS OF EPISODIC FLOODS, DROUGHTS, TURBIDITES ON ORGANIC CARBON BURIAL OVER THE PAST 2,000 YEARS IN THE SANTA BARBARA BASIN, CALIFORNIA

by

Caitlyn Sarno

Bachelor of Science
University of Delaware, 2016

Submitted in Partial Fulfillment of the Requirements

For the Degree of Master of Science in

Marine Science

College of Arts and Sciences

University of South Carolina

2019

Accepted by:

Claudia Benitez-Nelson, Director of Thesis

Lori Ziolkowski, Reader

Catherine Davis, Reader

Ingrid Hendy, Reader

Cheryl L. Addy, Vice Provost and Dean of the Graduate School

ACKNOWLEDGEMENTS

I would like to thank my advisor, Dr. Claudia Benitez-Nelson, for her support, understanding and helpful feedback throughout the past two years. I would also like to thank my committee for their support: Dr. Lori Ziolkowski for her career advice and lab guidance, Dr. Kate Davis for her helpful comments and perspective, and Dr. Ingrid Hendy for sharing her samples, data, and suggestions to make the project great. Additionally, I would like to thank past and previous members of the Benitez-Nelson/Moore lab for their continuous love and support: Shep, Meryssa, Blaire, Cameron, Callie, Phoebe, Katie, Jess, and Kelly. I would like to give an extra thank you to Pheobe (My) Le for her help running splitting all 1,500 samples and helping me run columns. I would like to thank my mom, dad, and David for their continuous support, and encouragement.

ABSTRACT

Over the past several millennia, Southern California has experienced episodic climate that have influenced the magnitude and composition of terrestrial and marine material that ultimately reaches ocean sediments. Here, we analyze elemental concentrations, stable isotopes, and n-alkane lipids as tracers of terrestrial and marine sources in drought, turbidite, and flood horizons from a well-dated sediment core in the Santa Barbara Basin (SBB) that spans the last 2,000 years. Stable isotopes ($\delta^{13}C$ and $\delta^{15}N$), indicate that more terrestrial organic carbon (OC) input occurred during floods relative to non-event periods, while bulk C/N ratios remained relatively constant (~10). Long chain n-alkanes, (C_{27}, C_{29}, C_{31}, C_{33}), characteristic of terrestrially derived OC, dominated all sediment types, but were 4 times more abundant during floods. Although relatively small in contribution to total OC burial, macrophytes (C_{21}, C_{23}) and marine algae (C_{15}, C_{17}, C_{19}) also contributed 4 and 3 times more to flood sediments compared to non-event sediments, respectively. Turbidites had three times as much algal and macrophyte n-alkanes and twice as much terrestrial *n*-alkanes relative to non-event sediment. Drought sediment, on the other hand, was distinguishable from non-event sediment only by higher $\delta^{15}N$ signatures. Combined, our data indicate that 8% of the total OC buried over the past 2,000 years occurred during 11 flood events, with 10% of deep sediment OC burial derived from shelf remobilization during 6 turbidite events. Comparison with modern day flooding suggests the large OC burial in flood sediments

came from megafloods. Overall, our work confirms that flood events transport and bury significant terrestrially derived OC on continental shelves.

TABLE OF CONTENTS

LIST OF TABLES

LIST OF FIGURES

LIST OF ABBREVIATIONS

BDL.....Below Detection Limit

C/N..... Carbon/Nitrogen

C_{15}, C_{17}, C_{19}..... Algal n-Alkanes

C_{21}, C_{23}..... Marine Macrophyte n-Alkanes

C_{27}, C_{29}, C_{31}..... Terrestrial n-Alkanes

CPI .....Carbon Preference Index

DCM .....Dichloromethane

ENSO .....El Niño Southern Oscillation

ETNP.....Eastern Tropical North Pacific

MeOH ..... Methanol

OMZ.....Oxygen Minimum Zone

PDO.....Pacific Decadal Oscillation

SBB .....Santa Barbara Basin

SXRF.....Scanning X-Ray Fluorescence

TN .....Total Nitrogen

TOC..... Total Organic Carbon

CHAPTER 1

INTRODUCTION

Marine sediments provide a window into Earth's climate over the geologic past and are useful for understanding and predicting future environmental change. Sediment composition and accumulation rate provide information regarding source(s) of organic carbon, sea surface temperature, precipitation, pH, and water column biological productivity (Soutar et al., 1977; Brassell et al., 1986; Kennedy and Brassell, 1992; Bond et al., 1993). Marine sediments also elucidate regional to global oscillations in terrestrial hydroclimate (Langbein and Schumm, 1958; Schimmelmann et al., 1990). Furthermore, marine sediments, and coastal environments in particular, are a large geological repository of carbon, influencing global climate via the regulation of the greenhouse gas, carbon dioxide (Martin et al., 1987). Thus, understanding the sources of organic carbon buried in marine sediments (e.g., terrestrial versus marine) provides insight into how coastal ecosystems influence carbon sequestration.

1.1 Study Site

Southern California often experiences floods and droughts due to its Mediterranean climate and response to the El Niño Southern Oscillation (ENSO) and Pacific Decadal Oscillation (PDO) (Barron et al., 2015). During the warm phases of ENSO and PDO, there is an increase in precipitation, river discharge, and presumably the amount of terrestrial sedimentation in SBB (Hendy et al., 2015). In addition, these warm

phases are associated with increased transport of warm, nutrient-depleted water from the subtropics with subsequent reduced marine productivity. ENSO and PDO change precipitation patterns that produce floods (warm phase) and droughts (cold phase) in the SBB region (Barron et al., 2010). The western coast of the US is vulnerable to floods of extremely hazardous proportions, termed megafloods (Dettinger and Ingram, 2013). These megafloods are thought to be caused by excessive rain from atmospheric rivers that may be further enhanced by ENSO and transport warm tropical water to mid latitudes (Dettinger and Ingram, 2013). More often, atmospheric rivers occur on smaller scales and are responsible for delivering 30-50% of the annual precipitation to the California region (Dettinger and Ingram, 2013).

The Santa Barbara Basin (SBB) is an optimal environment for paleoclimate reconstructions due to its suboxic nature and high sedimentation rate (Soutar et al., 1977; Hendy et al., 2013). SBB is located off the southern coast of California where it is encompassed by mountains on the northern side and islands on the southern side (Figure 1.1). There are two sills on the western and eastern sides of the basin that restrict water circulation of the bottom 100 meters of the basin. This lack of water circulation restricts the introduction of oxygen in bottom waters, creating a suboxic environment at a depth below 480 m that overlies anoxic sediments (Li et al. 2009). The anoxic sediment minimizes bioturbation and results in sediments that are ideal for high resolution age models using either varve counting or radiometric techniques (Hülsemann and Emery, 1961; Hendy et al., 2013). Highly refined age models have been developed for SBB sediments, thus there is an opportunity to examine episodic regional climate events, such

as floods and droughts over thousands of years (Soutar et al., 1977; Schimmelmann et al., 2003).

Annually, there are two main periods of sedimentation in the SBB that are visually differentiated by color. During the winter seasons, both the North Pacific High and the Jet Stream migrate south, strengthening the Aleutian Low and causing mild, wet, and stormy conditions in the region (Barron et al., 2010). These wet conditions tend to increase river discharge so that sediments presumed to be terrestrially derived are transported into the basin (Hülsemann and Emery, 1961; Thunell et al., 1995; Hendy et al., 2013). During the spring/summer, the North Pacific High and North American Low produce strong northwesterly winds that induce upwelling in the SBB and support high biological productivity (Hülsemann and Emery, 1961; Thunell et al., 1995; Hendy et al., 2013). As a result phytoplankton debris, dominated by diatoms (opal) and foraminifera (calcium carbonate), ultimately reach the basin bottom and are buried (Barron et al., 2010). Biogenic sediment is typically larger and can enhance clay sedimentation by flocculation of clays onto marine snow. Additional sources of sedimentary material in the spring/summer may also include benthic bacterial mats (e.g., *Beggiatoa*) that form after winter terrestrial inputs (Soutar and Crill, 1977), or in response to annual oxygenation of the basin during upwelling periods (Reimers et al. 1990; Bograd et al., 2002). Together, one terrigenous-rich and one biogenic-rich sediment lamina are assumed to represent a single year.

During a flood event, there is rapid transport of lithogenic sediment to the basin and annual laminae are replaced by a thick, gray flood layer (Barron et al., 2015). This thick, gray flood layer is similar, but not to be confused with turbidites. Turbidite

formation is distinctively different from flood layer in that they occur in response to flood movement (Du et al., 2018), and transport sediment from the shelf into the basin. Turbidites are visually distinct from flood deposits and are characterized by an olive coloration and differences in grain size (Schimmelmann et al., 1998; Hendy et al., 2013).

1.2 Geochemical Tools

The impact of episodic flood, turbidite and drought on carbon burial in the SBB have yet to be investigated. This study utilized several sedimentary geochemical tools including stable isotopes ($\delta^{13}C$, $\delta^{15}N$) of bulk sediments, total organic carbon (TOC) and nitrogen (TN) concentrations, and *n*-alkane lipid biomarker concentration, to determine sediment composition within flood, turbidite, drought, and non-event layers. Carbon to nitrogen (C/N) ratios provide a broad view of organic matter source, where C/N ratios > 20 are indicative of the structural material needed by land plants (Hedges et al., 1986). However, C/N ratios are often imprecise due to the mixing of multiple sediment inputs (rivers, marine algae, vascular plants, etc.). As such, organic matter stable isotopes are also used to determine sediment source. In terrestrial environments, the isotopic composition of plants is usually depleted in the heavier isotopes (i.e., $\delta^{13}C_{terrestrial}$= -27‰ and $\delta^{15}N_{terrestrial}$ = 2‰), while marine sources tend to have a higher isotopic signal ($\delta^{13}C_{marine}$= -20‰ and $\delta^{15}N_{marine}$ = 10‰) (Sweeney and Kaplan, 1980; Meyers, 1994).

While C and N isotopes may distinguish organic matter source (marine versus terrestrial), these isotopes also undergo additional fractionation processes both in the water column and on land. Surface water entering SBB during the summer months flows northward from the Eastern Tropical North Pacific (ETNP) and has a higher $\delta^{15}N$ value

(Voss et al., 2001; Brandes Jay et al., 2003; Sigman et al., 2003). In the winter and spring, strong winds stimulate upwelling of nutrient enriched waters, potentially resulting in sinking organic matter lower in $\delta^{15}N$ as organisms preferentially utilize the lighter isotopes of N. This process leaves waters enriched in heavy isotopes. However, as waters become increasingly nutrient depleted, organisms will reduce their discrimination against specific isotopes during uptake and sinking organic matter will contain higher $\delta^{15}N$. Other processes that may fractionate nitrogen in the basin include denitrification, a process converts nitrate in nitrogen gas, by utilizing nitrate as a terminal electron acceptor in respiration in place of oxygen. Denitrification can raise the $\delta^{15}N$ signal of the water body as the lighter nitrogen isotope is preferentially utilized to form nitrogen gas, leaving behind an enriched pool of nitrogen (Emmer and Thunell, 2000). On the other hand, carbon isotopes are differentially fractionated by C3 and C4 metabolic processes, making it difficult to distinguish terrestrial sources from marine algae if the terrestrial source is comprised of high proportions of C4 plants (Meyers, 1994).

Given the multitude of controls on the isotopic composition of sediment, biomarkers can be used to further distinguish sediment source (Blumer and Clark, 1967). Biomarkers are molecular compounds characteristic of a specific organism under a particular set of environmental conditions. The biomarkers used in this study degrade very slowly, keeping their molecular structure intact over long timescales and allowing for the source of a material to be determined by using its molecular structure. Here, we focused on *n*-alkanes as they are generally unreactive, degrade slowly overtime, and chain length reflects source. Terrestrial vegetation is characterized by long chain *n*-alkanes (C_{27}, C_{29}, C_{31}, C_{33}) which are utilized for protection and support in leaf waxes

(Meyers, 2003; Ficken et al, 2000). On the other hand, marine phytoplankton are characterized by short chain *n*-alkanes (C_{15}, C_{17}, C_{19}) and marine macrophytes by mid-chain length *n*-alkanes (C_{21}, C_{23}, C_{25}) (Meyers, 2003; Ficken et al, 2000). By measuring the distribution of *n*-alkanes in sediment, the relative contribution from marine and terrestrial sources can be determined. The objective of this study was to analyze the TOC, TN, the C/N ratio, $\delta^{13}C$ and $\delta^{15}N$ isotopes, and *n*-alkane biomarkers of a well-dated sediment core collected from the center of SBB (previously age dated by Hendy et al., 2013) to elucidate the source of organic matter to marine sediments during episodic events (e.g., floods, turbidites, and droughts) over the past 2000 years. Understanding the composition of organic matter in these sediments deposited under different climate conditions provides information about how coastal ecosystems influence carbon sequestration.

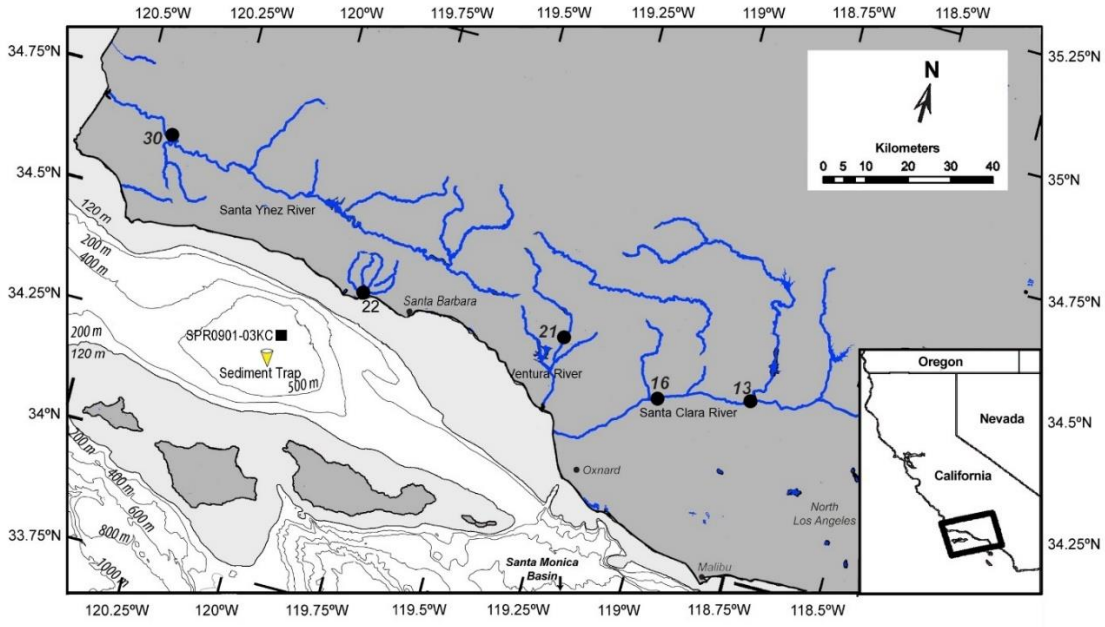

Figure 1.1: Map of the Santa Barbara Basin (SBB). The sediment core is labelled as the black square (34°16.99'N, 120°2.41'W), the sediment trap is the yellow triangle (34°14′N, 120°02′W), and the river sites are the black circles: Santa Clara River, stations 13 (34˚23.10' N, 118˚47.22'W), station 16 (34˚20.70'N, 119˚01.46'W); Ventura River, station 21 (34˚25.20'N, 119˚ 17.94'W); Santa Ynez River, station 22 (34˚24.60'N, 119˚49.74'W), station 30 (34˚38.40'N, 120˚24.54'W). River sites are from Napier et al. (2019).

CHAPTER 2

METHODS

2.1. Collection and Dating

A sediment core (SPR0901-03KC; 34°16.99'N, 120°2.41'W) was collected from the SBB in January 2009 at a water depth of 586 m (Hendy et al., 2013). Flood and turbidite layers, and drought intervals, were identified from elemental analyses with Scanning X-Ray Fluorescence (SXRF) (Hendy et al., 2015; Heusser et al., 2015), with flood sediments comprised of high concentrations of lithogenic elements such as titanium, potassium, iron and calcium, and droughts comprised of low lithogenic element concentrations. Turbidites were identified by their olive homogenous coloration and larger grain size (Schimmelmann et al., 1998; Hendy et al., 2013; Du et al, 2018). After scanning the core, it was sampled 2 mm intervals and oven dried. An age model was developed using a combination of ^{14}C dating of planktonic foraminiferal carbonates and laminae counts (Hendy et al., 2013).

Terrestrial end members were defined with river sediment previously collected from dry stream beds during the drought of 2013-2016 (Napier et al., 2019). (Figure 1.1). River sediment from 5 locations were analyzed: the Santa Clara River was sampled at locations 13 (34˚23.10' N, 118˚47.22'W) and 16 (34˚20.70'N, 119˚01.46'W); the Ventura River was sampled at location 21 (34˚25.20'N, 119˚ 17.94'W); the Santa Ynez River was sampled at locations 22 (34˚24.60'N, 119˚49.74'W) and 30 (34˚38.40'N, 120˚24.54'W) as described in Napier et al., (in press). The macrophyte end member was

defined by a sample of kelp that was collected from Coal Oil Point in June 2018. Samples were shipped to the University of South Carolina where they were freeze dried and ground prior to analysis.

Sediment traps were utilized to compare core events to modern day flood and non-event sediment to paleo-floods. The sediment traps were deployed in the center of the SBB (34°14′N, 120°02′W; Figure 1.1) at a depth of 500 m in 1993 and continue to present day (Thunell, 1998). Sediment trap flood samples were selected from the 1997-1998 El Niño flood collected in March-April 1998. Sediment trap non-event samples from after the El Niño were selected based on their lack of flood, drought or turbidite events in November 2000 and November 2001.

2.2. Total Organic Carbon, Total Nitrogen, and Isotopic Measurements

The weight percent of total organic carbon (%OC) and organic nitrogen (%ON) was measured on a Perkin Elmer 2400 CHNS Elemental Analyzer. The standard deviation of TOC and TN measurements for standard replicates was 0.03% and 0.04%, respectively. For OC analyses, inorganic carbon was removed by acidifying 0.5 mg of sediment with 6 mL of 1 M phosphoric acid, sonicating for 5 minutes, and filtering onto a precombusted GF/F. The filters were dried overnight, folded into 3.0 cm tin disk and pelletized for analysis. For isotopic analysis of C and N, samples were combusted in a Eurovector Elemental Analyzer connected to an Elementar Isoprime IRMS. Reference material for ^{13}C were USGS-24, USGS-40, and sucrose. Reference material for ^{15}N were IAEA-N1 and N2 (ammonium sulfates) and USGS-40. Isotopic measurements are given

in reference to a standard; $\delta^{13}C$ was reported relative to Vienna Pee Dee Belemnite (VPDB) and $\delta^{15}N$ was reported relative to atmospheric nitrogen (0‰).

2.3. n-Alkane Analyses

Approximately 2 g of homogenized and dried sediment or kelp were used for lipid extraction. Given the large amount of material needed, multiple core intervals of similar isotopic nitrogen signatures were pooled, encompassing ~ 1 y for flood and turbidite samples and ~ 8 y for non-event and drought samples. Lipids were extracted in triplicate by sonicating for 30 min in 50 mL of a 9:1 dichloromethane/methanol (DCM/MeOH) solution and filtering through a GF/F. The extract was concentrated to 2 mL via evaporation under ultrahigh purity nitrogen gas. Sulfur was removed from samples by adding ~ 500 mg activated copper and allowing samples to stand overnight.

The *n*-alkanes were separated from the total lipid extract with silica gel column chromatography using a modification of Li et al. (2009). The column was packed with 7 cm of silica gel in DCM and 1 cm of anhydrous sodium sulfate to prevent aqueous contamination. The column was made with DCM to minimize contamination that arose from hexane extracting atmospheric contaminants. To switch to a hexane column, the column was loaded with 40 mL of hexane before loading the sample. Once the sample was added, the first fraction (40 mL hexane) was collected for hydrocarbon analysis. This hydrocarbon fraction was evaporated to 500 µL under ultrahigh purity nitrogen gas and analyzed with a GC/MS. The remaining fractions were stored for future analysis of ketones/esters (40 mL 4:1 hexane/DCM), alcohols (40 mL 9:1 DCM/acetone), and fatty acids (40 mL 12:12:1 DCM/MeOH/Formic Acid).

n-Alkanes were identified and quantified using an Agilent 7890B/5977A GC/MS with HP-5MS column outfitted with UHP helium as a carrier gas. One µL of sample was injected into the GC/MS on splitless mode. The initial column temperature was 100℃, increased at a rate of 8℃ min^{-1} until 300℃, and remained at 300℃ for 23 min. *n*-Alkanes were detected utilizing scanning ion monitoring (SIM) targeting the m/z ion 71. *n*-Alkanes were identified using external standards of known retention times and by analysis of the SIM chromatograms. *n*-Alkane concentrations were determined using external standards (C_{20}, C_{24}, C_{26} and C_{30}) and extrapolating the slopes for the other *n*-alkane chain lengths.

A carbon preference index (CPI) was utilized as a proxy for fresh organic carbon (Bray and Evans, 1961). In this study, a modified CPI equation (Pearson and Eglinton, 2000; Scanlan and Smith, 1970; Bray and Evans, 1961), was used to encompass the entire spectrum of contributing *n*-alkanes (Eq 1). The numerator in this equation is the sum of the concentration (µg/gOC) of all odd chain *n*-alkanes from 13 to 33 carbon atoms in length, and the denominator is the sum of the concentration of all even chain *n*-alkanes from 14 to 32 carbon atoms in length. Previous work has shown that a higher CPI indicates a greater contribution from fresh organic carbon sources (Bray and Evans, 1961). A lower CPI and increased abundance of even chain *n*-alkanes derive from bacterial degradation and petroleum (Bray and Evans, 1961; Grimalt et al., 1985).

Equation 1: $$CPI = \frac{C_{13}+C_{15}+C_{15}+C_{17}+C_{19}+C_{21}+C_{23}+C_{25}+C_{27}+C_{29}+C_{31}+C_{33}}{C_{14}+C_{16}+C_{18}+C_{20}+C_{22}+C_{24}+C_{26}+C_{28}+C_{30}+C_{32}}$$

2.4. Statistical Analysis

Significant differences between samples were determined using a one tailed Student's t-test assuming unequal variances where $\alpha < 0.05$. These statistical analyses allowed for gross characterization of events (i.e. flood versus non-event). While this study may suggest transport mechanisms to the ocean floor, we did not account for any transformations that may have occurred in the water column. We also assume that there was no preferential degradation of specific *n*-alkanes within the water column or sediment.

CHAPTER 3

RESULTS

Flood events were identified in the sediment core by SXRF as having high concentrations of lithogenic elements, Ti and Fe, and low concentrations of the biogenic element, Ca (Hendy et al., 2015; Du et al, 2018). Drought intervals were identified by low concentrations of lithogenic elements and high concentrations of biogenic elements (Hendy et al., 2015). Turbidite sediment was characterized its homogenous olive coloration and larger grain size, and were thought to be derived from turbidity currents stimulated by a mass failure on the shelf (Schimmelmann et al., 1998; Hendy et al., 2015; Du et al, 2018). Non-event sediment was selected based on the absence of properties characteristic of flood or turbidite events.

3.1. TOC, TN, C/N, and Isotopic Results

Flood sediment (n = 20) had an average TOC of 1.32 ± 0.12% and TN of 0.16 ± 0.02% (Table 3.1). Non-event sediment (n =11) had a significantly higher TOC of 2.75 ± 0.19% and TN of 0.32 ± 0.02% ($P < 0.01$). The C/N ratio remained constant for both non-event (10.01 ± 0.76) and flood sediment (9.93 ± 0.32). Flood sediment was characterized by significantly lower $\delta^{13}C$ (-24.34 ± 0.29‰) and $\delta^{15}N$ (6.47 ± 0.95‰) relative to non-event samples ($p < 0.01$). The isotopic data paired with the floods identified previously with SXRF showed excellent agreement (Hendy et al., 2015) (Figure 3.1).

Typically, the sedimentation rate for the SBB non-event sediment was 0.98 ± 0.17 mm y^{-1} and the OC burial rate was 3.34 ± 0.47 mg cm^{-2} y^{-1}(Table 3.2). However, the sedimentation rate significantly increased for both flood ($p = 0.01$) and turbidite sediments ($p = 0.01$). The sediment accumulation rate for flood sediment was 29 ± 32 mm y^{-1} and had an OC burial rate of 59 ± 63 mg cm^{-2} y^{-1}. The sedimentation rate for turbidities was 50 ± 32 mm y^{-1} and an OC burial rate of 134 ± 104 mg cm^{-2} y^{-1}.

Other notable sediment intervals in our sediment core were turbidites and droughts. Turbidites had a TOC of 2.07 ± 0.34% that was similar to the TOC measured during flood events and a TN concentration of 0.27 ± 0.02% fell just below the non-event TN values. Turbidite C/N ratios of 8.90 ± 0.59. While turbidites were characterized by a $\delta^{15}N$ signature of 7.62 ± 0.21‰, similar to non-event sediment, the $\delta^{13}C$ signature of -22.57 ± 0.25‰, was much lower than both flood and non-event sediment. Meanwhile, drought intervals were nearly indistinguishable from non-event sediment. Their TOC was 2.68 ± 0.16%, TN was 0.34 ± 0.01%, and their C/N ratio averaged 9.12 ± 0.31. Droughts also had a similar $\delta^{13}C$ = -22.26 ± 0.02‰, but a significantly higher $\delta^{15}N$ = 7.94 ± 0.09‰ compared to the non-event sediment ($p=0.003$).

Sediment from each of the rivers were measured to constrain the terrestrial end member. The C/N ratios for each river were similar, 9.9 ± 1.6. However, the isotopic composition differed where $\delta^{13}C$ ranged from -31.53‰ to -22.80‰ and $\delta^{15}N$ ranged from 4.41‰ to 8.51‰ (Table 3.3). Kelp samples were also measured to constrain the input of macrophytes to the basin and were characterized by a C/N ratio of 15.45, a higher $\delta^{13}C$ of -14.73‰ and $\delta^{15}N$ of 9.79‰.

Sediment trap samples collected during and after the 1997-1998 El Niño were analyzed to constrain recent flood and non-event source signatures in the SBB. Sediment trap TOC (non-event: 3.97%, flood: 3.53%) and TN (non-event: 0.53%, flood: 0.52%) concentrations were much higher than those measured in the sediment core due to the relative freshness of the material. Sediment trap C/N ratios (non-event: 8.75, flood: 7.91) were similar to the C/N ratio measured throughout the sediment core. The $\delta^{15}N$ of the non-event, 7.87‰, and flood, 6.62‰, sediment trap samples were comparable to sediment core non-event and flood sediment.

3.2. n-Alkanes

The *n*-alkane composition was used to characterize the terrestrial end member through river samples and the macrophyte end member through a kelp sample. All river samples confirmed previously reported terrestrial *n*-alkane composition by consisting of 94-100% long chain *n*-alkanes (Santa Clara River 147 ± 1 µg/gOC, Santa Ynez River 155 ± 37µg/gOC, and Ventura River 820 µg/gOC) (Table 3.4) (Meyers, 2003; Ficken et al, 2000). Both the Santa Clara and Santa Ynez Rivers also contained the *n*-alkane, C_{25}, most likely due to river macrophytes that the Ventura River lacked. Kelp samples contained midchain *n*-alkanes, C_{21} and C_{23}, but did not contain C_{25}. Therefore, we excluded C_{25} from our marine macrophyte end member analyses.

Flood events were characterized by increased *n*-alkane concentrations (Figure 3.2, Figure 3.3, Figure 3.4). There was a significant increase in terrestrial *n*-alkane (C_{27}, C_{29}, C_{31}, C_{33}) concentrations in flood (105 ± 47 µg/gOC) compared to non-event (27 ± 18 µg/gOC) sediment ($p < 0.001$) (Table 3.4; Figure 3.2). Flood events were also

characterized by significantly greater concentrations of macrophyte *n*-alkanes (C_{21}, C_{23}) (8 ± 10 µg/gOC) ($p = 0.05$) and higher concentrations (17 ± 19 µg/gOC) of algal *n*-alkanes (C_{15}, C_{17}, C_{19}) compared to non-event sediment (6 ± 5 µg/gOC) ($p = 0.03$) (Figure 3.2). Furthermore, the lower $\delta^{15}N$ isotopic signatures were in agreement with higher concentrations of representative biomarker *n*-alkanes, the terrestrial *n*-alkane, C_{29}, the macrophyte *n*-alkane, C_{21}, and the algal *n*-alkane, C_{17} (Figure 3.2). Flood events were also characterized by greater CPI ratios relative to non-event sediment; 3.62 ± 1.77 versus 2.25 ± 2.13, respectively but the high variability resulted in a lack of significance ($p = 0.08$).

Turbidite *n*-alkane composition was most similar to non-event sediment, but still had some flood sediment characteristics (Table 3.4; Figure 3.3). Turbidites generally had greater concentrations of terrestrial *n*-alkanes (46 ± 23 µg/gOC) ($p = 0.06$) and algal *n*-alkanes (16 ± 8 µg/gOC) compared to the non-event ($p = 0.01$). Turbidites also had a macrophyte concentration (6 ± 5 µg/gOC) similar to both the non-event ($p = 0.08$) and flood sediment ($p = 0.31$).

The *n*-alkane composition of drought sediment was indistinguishable from non-event sediment; terrestrial *n*-alkanes (20 ± 9 µg/gOC; $p = 0.24$), macrophyte *n*-alkanes (2 ± 2 µg/gOC; $p = 0.49$), algal *n*-alkanes (7 ± 4 µg/gOC; $p = 0.38$).

Sediment trap samples were dominated by terrestrial *n*-alkanes (non-event 29 ± 6 µg/gOC; flood 40 ± 24 µg/gOC, $p = 0.37$) followed by a large contribution of algal *n*-alkanes (non-event 19 ± 14 µg/gOC; flood 27 ± 8 µg/gOC, $p = 0.33$) (Figure 3.3). Macrophyte *n*-alkane concentrations, however, were low for both flood and non-event sediment traps (non-event 4 ± 4 µg/gOC; flood BDL, $p = 0.25$). Overall, sediment traps

had higher abundances of algal and terrestrial *n*-alkanes compared to the sediment core non-event which we attributed to shorter time available for degradation (Figure 3.3).

Table 3.1: Accumulation of TOC, TN, Isotopic Results

	Non-Event n=12	**Flood** n=20	**Turbidite** n=6	**Drought** n=3	**Kelp** n=1	**Sediment Trap Baseline** n=2	**Sediment Trap Flood** n=2	**Santa Clara River** n=2	**Santa Ynez River** n=2	**Ventura River** n=1
TOC (wt %)	2.75 ± 0.12	1.32 ± 0.19	2.07 ± 0.34	2.68 ± 0.16	13.79	3.97 ± 0.18	3.53 ±1.32	1.56 ± 1.12	1.64 ± 0.49	0.87
TN (wt %)	0.32 ± 0.02	0.16 ± 0.02	0.27 ± 0.02	0.34 ± 0.01	1.04	0.53 ± 0.05	0.52 ± 0.22	0.16 ± 0.09	0.17 ± 0.02	0.12
C/N	10.01 ± 0.76	9.93 ± 0.32	8.90 ± 0.59	9.12 ± 0.31	15.45	8.75 ± 0.45	7.91 ± 0.40	10.06 ± 2.43	11.35 ± 1.94	8.23
$\delta^{13}C$ (‰)	-21.75 ± 0.18	-24.34 ± 0.29	-22.57 ± 0.25	-22.26 ± 0.02	-14.73	-21.01 ± 0.45	-22.12 ± 0.12	-28.15 ± 3.38	-25.53 ± 1.50	-22.8
$\delta^{15}N$ (‰)	7.65 ± 0.24	6.47 ± 0.95	7.62 ± 0.21	7.94 ± 0.09	9.79	7.87 ±14	6.62 ± 0.15	7.76 ± 0.76	6.29 ± 0.01	4.41

Table 3.2: Sedimentation and Burial Rates

	Sedimentation Rate (mm/y)	**OC Burial Rate (mg cm^{-2} y^{-1})**	**Terrestrial Burial Rate (µg/cm^{-2}/y^{-1})**	**Macrophyte Burial Rate (µg/cm^{-2}/y^{-1})**	**Algal Burial Rate (µg/cm^{-2}/y^{-1})**
Non-Event	0.98 ± 0.17	3.34 ± 0.47	0.09 ± 0.06	0.01 ± 0.01	0.02 ± 0.02
Flood	29 ± 32	59 ± 63	7.83 ± 8.91	0.44 ± 0.69	0.86 ±1.22
Turbidite	50 ± 32	134 ± 104	3.58 ± 2.91	0.20 ± 0.27	1.37 ± 0.94
Drought	0.93 ± 0.16	3.29 ± 0.41	0.07 ± 0.03	0.01 ± 0.01	0.02 ± 0.02

Table 3.3: River End Member Composition

Location Number **River**	**13** **Santa Clara**	**16** **Santa Clara**	**21** **Ventura**	**22** **Santa Ynez**	**30** **Santa Ynez**
Latitude, **Longitude**	34°23.10'N 118°47.22'W	34°20.70'N 119°01.46'W	34°25.20'N 119°17.94'W	34°24.60'N 119°49.74'W	34°38.40'N 120°24.54'W
C_{25} (µg/gOC)	5.89	BDL	BDL	7.05	11.66
Terrestrial C_{27}, C_{29}, C_{31} (µg/gOC)	147	146	820	118	192
TOC	2.68	0.43	0.87	2.13	1.15
TN	0.25	0.07	0.12	0.19	0.14
C/N	12.49	7.62	8.23	13.29	9.41
$\delta^{13}C$ (‰)	-24.77	-31.53	-22.80	-27.10	-24.05
$\delta^{15}N$ (‰)	7.00	8.51	4.41	6.28	6.30

Table 3.4: Accumulation of *n*-Alkane Results

	Non-Event n=7	**Flood** n=11	**Turbidite** n=5	**Drought** n=3	**Kelp** n=1	**Sediment Trap Baseline** n=2	**Sediment Trap Flood** n=2	**Santa Clara River** n=2	**Santa Ynez River** n=2	**Ventura River** n=1
CPI	2.25 ± 2.13	3.62 ± 1.77	4.11 ± 4.95	4.02 ± 3.36	2.12	5.96 ± 2.34	3.33 ± 1.12	Only Odds	Only Odds	Only Odds
Algal C_{15}, C_{17}, C_{19} (µg/gOC)	6 ± 5	17 ± 19	16 ± 8	7 ± 4	16	19 ± 14	27 ± 8	BDL	BDL	BDL
Macrophyte C_{21}, C_{23} (µg/gOC)	2 ± 4	8 ± 10	6 ± 5	2 ± 2	7	4 ± 4	BDL	BDL	BDL	BDL
Terrestrial C_{27}, C_{29}, C_{31} (µg/gOC)	27 ± 18	105 ± 47	46 ± 23	20 ± 9	BDL	29 ± 6	40 ± 24	147 ± 1	155 ± 37	820

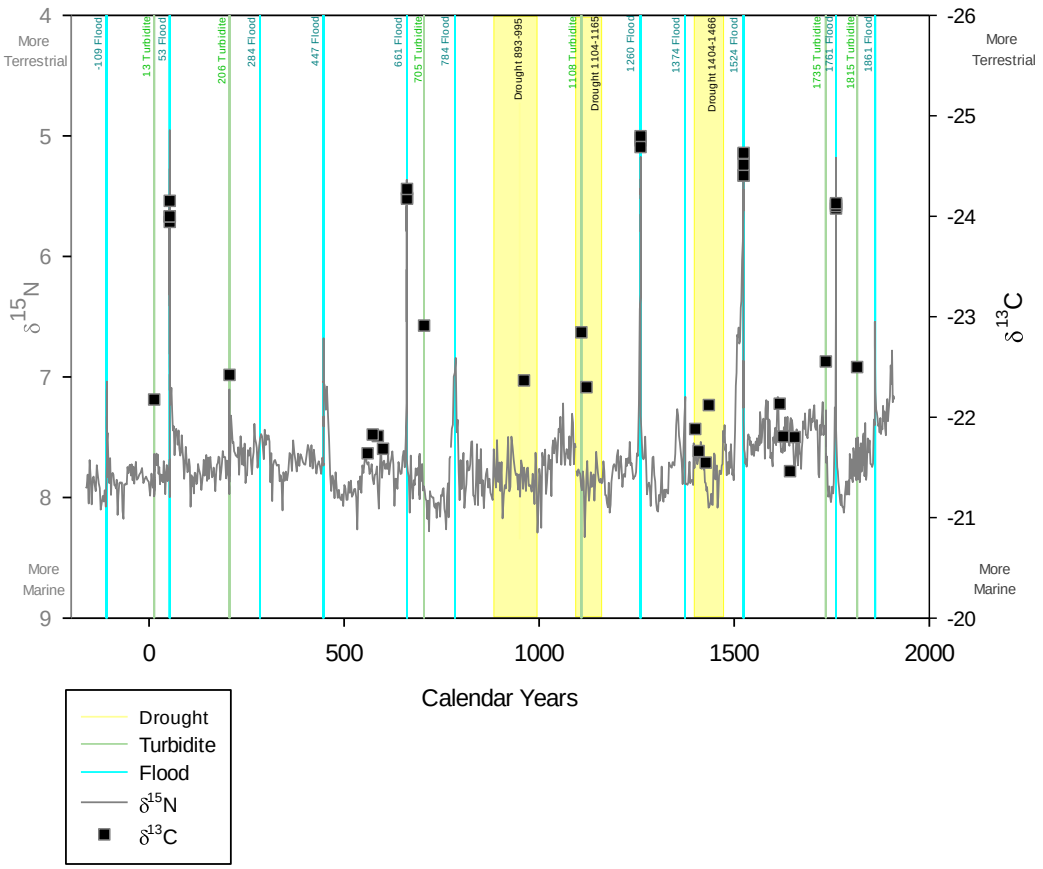

Figure 3.1: A time series of the past 2,100 years depicting decreases in $\delta^{13}C$ and $\delta^{15}N$ during floods (blue lines) previously identified with Scanning X-Ray Fluorescence (SXRF).

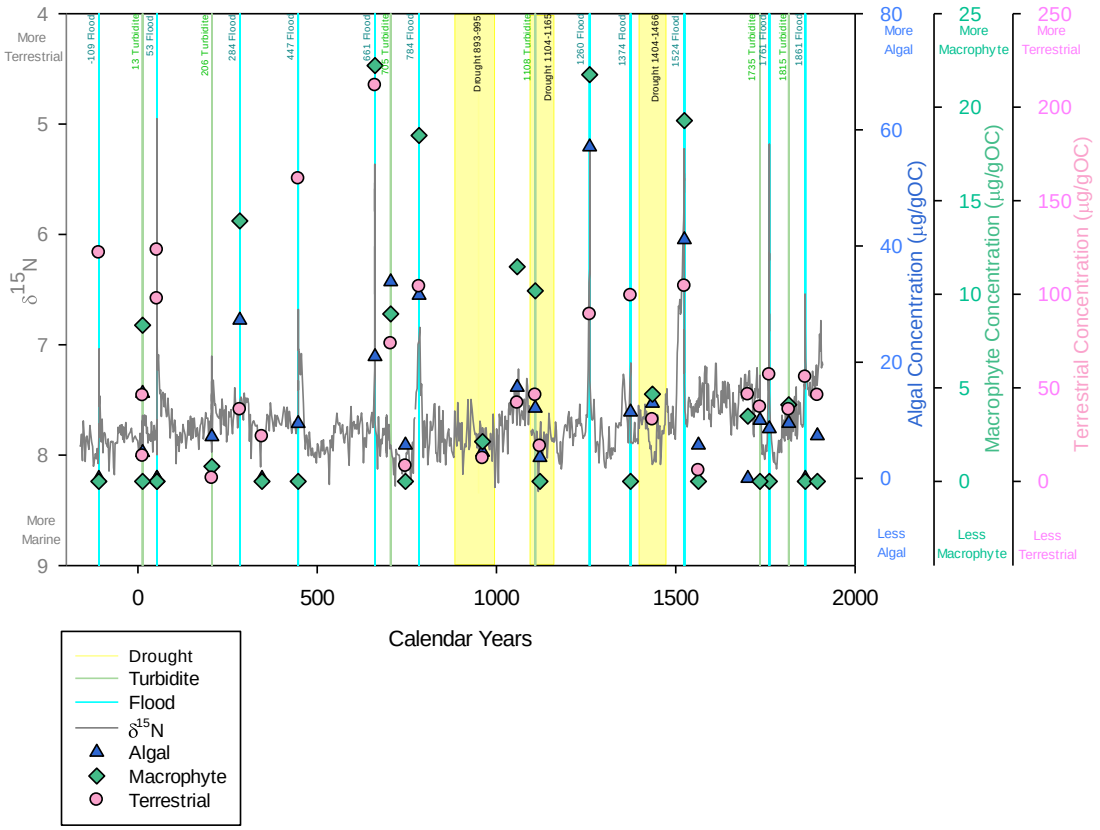

Figure 3.2: A time series of the past 2,100 years depicting decreases $\delta^{15}N$ and increases in *n*-alkanes during floods (blue lines) previously identified with Scanning X-Ray Fluorescence (SXRF).

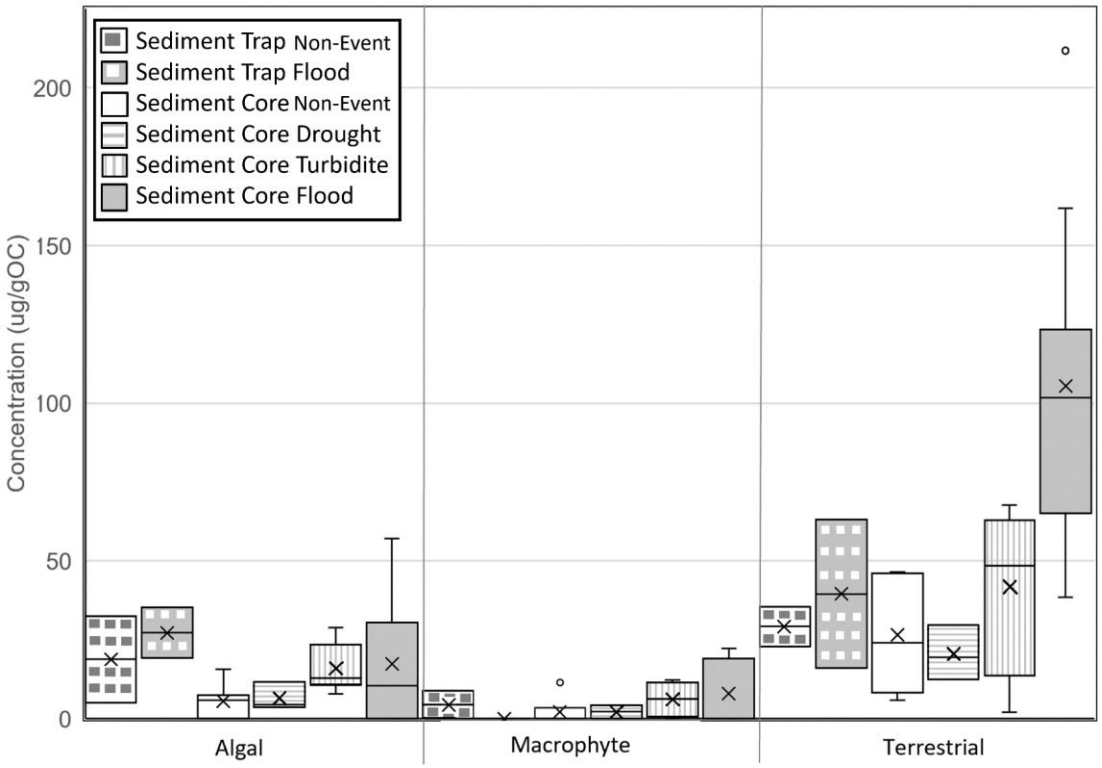

Figure 3.3: Carbon normalized *n*-alkanes in sediments dominated by terrestrial (C_{27}, C_{29}, C_{31}, C_{33}) sources relative to algal (C_{15}, C_{17}, C_{19}) and macrophyte (C_{21}, C_{23}) organic matter. Within each box, the line is the median, the X is the mean, and points outside of the box are outliers.

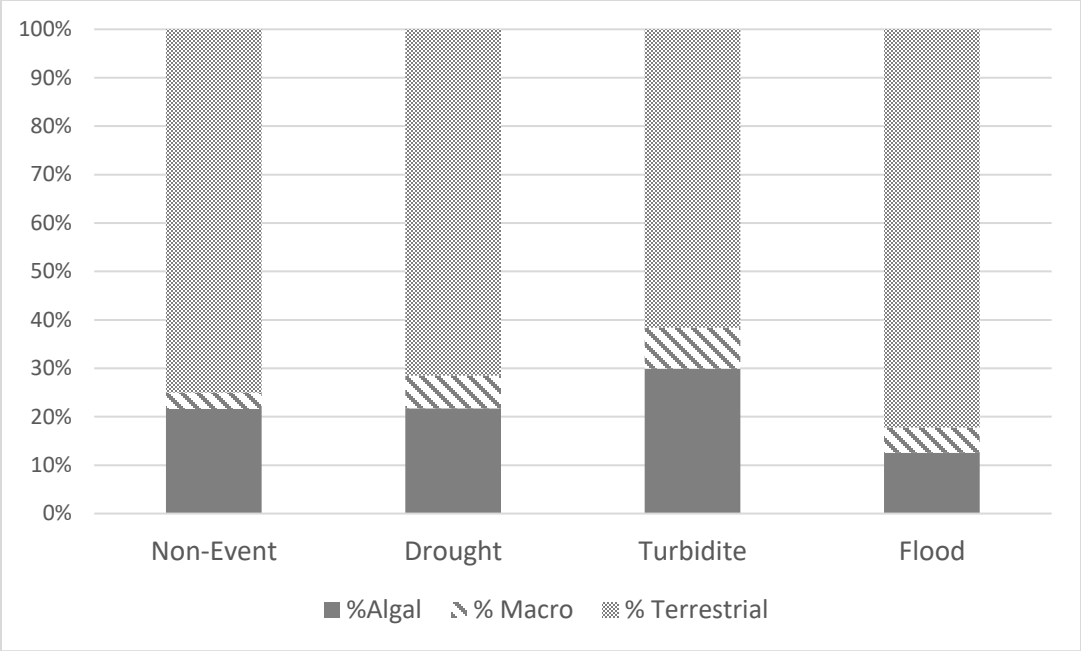

Figure 3.4: Contribution of *n*-alkanes in each type of sedimentation. All sediment was dominated by terrestrial *n*-alkanes, however, flood sediment had the greatest percentage (82%) of terrestrial *n*-alkanes.

CHAPTER 4

DISCUSSION

The burial of organic carbon in oceanic sediments is a major sequestration pathway of carbon dioxide on millennial to geologic timescales (Martin et al., 1987). The source of this organic carbon and mechanisms of delivery to sediments, however, are still being resolved. For example, small mountainous river systems on continental shelves, such as the SBB, may be an underestimated source of organic carbon. Recent studies suggest small mountainous river systems may deliver almost half the world's global particulate organic matter to coastal oceans (Hatten et al., 2010; Bao et al., 2015; Hedges and Keil, 1995). The SBB is sensitive to seasonal, regional (ENSO), and long-term climatic shifts (PDO) that are associated with more frequent floods (positive phase) and droughts (negative phase). Using the elemental composition of the sediments we identified 11 floods, 3 droughts, and 6 turbidites over the last 2,000 years (Hendy et al., 2015). Our isotopic and OC analyses of organic matter targeted these events in order to determine sediment source and composition as well as to further understand the impacts these events have on organic carbon burial.

During flood events, high precipitation rates lead to increased river discharge, which brings more terrestrial material into the continental margin and increases sedimentation rates. During flood events, average sedimentation rates increased to 29 mm y^{-1} and were as high as 115 mm y^{-1} (53 A.D.). In contrast, the sedimentation rate within

the SBB in non-event and drought sediment averaged 1 mm y^{-1} and is similar to previous work in the SBB (Emery and Hülsemann, 1962; Thunell, 1998; Emmer and Thunell, 2000). These flood sediments were comprised of TOC and TN concentrations that were about 50% lower than those measured during non-event periods, yet the C/N ratios were similar, 9.93 ± 0.32 and 10.01 ± 0.76 for flood and non-event sediments respectively. SBB is surrounded by rivers that drain mountainous terrain and have large catchment areas where soils undergo degradation. Thus, flood OM contains a lower C/N ratio characteristic of degraded OM versus fresh material (Goñi et al., 2013; Blair et al., 2003). Despite the lower TOC concentration, these flood events were still responsible for burying OC at a rate 17 times faster than non-event and drought periods.

The sedimentary process that emplaces turbidites remobilizes sediment from the shelf and transport it into the deep basin at a rate 40 times faster than the non-event sediment accumulation. On average, turbidites had sedimentation rates of 50 ± 32 mm y^{-1}, with a single event as high 95 mm y^{-1}, and these rates were comparable to previously measured sedimentation rates (Soutar et al., 1977). Turbidites had TOC (1.76) and TN (0.24) concentrations that fell between those of flood and non-event sediments. This suggests that turbidites are comprised of a mixture of lithogenic and degraded and fresh organic matter sources.

Over the past 2,000 years, non-event and turbidite periods were characterized by a relatively constant $\delta^{15}N$ of 7.65 ± 0.24‰. These results are similar to Emmer and Thunell (2000), who measured $\delta^{15}N$ over the past 50 kyr in SBB sediments from ODP Hole 893A. Over the past 15 kyr, they found an average $\delta^{15}N$ of 7.88‰ which reflects similar

sedimentation to the past 2,000 years(Emmer and Thunell, 2000). A $\delta^{15}N$ of 7.5‰ is consistent with a source of sinking organic matter derived from biological activity in oceanic surface water (Sweeney and Kaplan, 1980). Emmer and Thunell (2000) attributed variations of $\delta^{15}N$ to changes in nitrogen cycling within the water column, specifically water column denitrification occurring within the Eastern Tropical North Pacific (ETNP) delivered to SBB by water advected northward along the North American Margin. For example, a denitrification signal was detected over the past 150 years when the $\delta^{15}N$ of ETNP waters decreased ~1‰ from the non-event $\delta^{15}N$ of 7.65‰. Deutsch et al., (2014) attributed this decline to a deepening of the thermocline resulting from the weakening of the trade winds, which minimized respiration rates through reduced upwelling driven primary productivity. This reduced oxidant demand prevented expansion of the OMZ and reduced denitrification in the ETNP. Around 1980, the $\delta^{15}N$ subsequently increased in the SBB and was caused by a strengthening of the trade winds, shoaling the thermocline to allow nutrients back into surface water to increase respiration and expand the OMZ in the ETNP, and therefore increase denitrification (Deutsch et al., 2014; Cheung et al., 2016).

However, the denitrification fluctuation in $\delta^{15}N$ of 1‰ is still much smaller than the $\delta^{15}N$ variation during flood events, which can be as large as 2.5‰. Flood events were characterized by a much lower sediment isotopic composition ($\delta^{13}C$ = -24.34 ± 0.29‰; $\delta^{15}N$ = 6.47 ± 0.95‰) which suggested a large influence from terrestrial material. Previous studies have shown that terrestrial organic matter has a lower $\delta^{13}C$ and $\delta^{15}N$ isotopic signature compared to marine sources (Sweeney and Kaplan, 1980; Meyers, 1994). In the SBB, Sweeney and Kaplan (1980) conducted a $\delta^{15}N$ terrestrial end member

analysis by measuring terrestrial sewage effluent and found terrestrial $\delta^{15}N$ was ~2‰. Furthermore, river sediment was used as our terrestrial end member, and had a much lower isotopic composition. Similarities between the river sediment isotope composition (Table 3.1) and flood sediment isotopic composition suggested that flood sediment had a terrestrial source.

A seasonal trend in nitrogen isotopes further supports terrestrial input into the SBB (Thunell, 1998; Davis et al., *this issue*). Thunell (1998) found that lithogenic material was a significant source of organic matter to SBB sediments based upon sediments collected in deep moored sediment traps. Thunell (1998) proposed that lithogenic material was transported into the basin via two different mechanisms. The first mechanism occurred on a seasonal time cycle in association with spring blooms. Lithogenic particles, which typically have very small grain sizes and sink slowly, scavenge onto larger biogenic particles during the spring and thus sink rapidly to the seafloor (Thunell, 1998). Indeed, this hypothesis is supported by Davis et al. (*this issue*), who measured a lower $\delta^{15}N$ signal of in deep sediment trap material (500 m) during the spring bloom. The second mechanism suggested by Thunell (1998) was that lithogenic particles settled onto the margin and were subsequently carried to the center of the SBB by storms or wave activity. However, it is also known that lithogenic material can reach the basin through hyperpycnal flows from denser material flowing from the rivers during floods.

The isotopic composition of flood sediment suggest rivers are depositing terrestrial sediment to the basin. The Santa Clara, Ventura, and Santa Ynez Rivers all had

low $\delta^{13}C$ values characteristic of terrestrial sedimentation. Typically, the Santa Clara River is the dominant contributor of sediment to the SBB since it has the highest riverine discharge. However, the $\delta^{15}N$ of flood sediment was most similar to the $\delta^{15}N$ of the Santa Ynez and Ventura Rivers rather than the Santa Clara River. Therefore, our $\delta^{15}N$ results suggested that the Santa Ynez and Ventura Rivers play a larger role in contributing terrestrial sediment to SBB during floods than they do during non-event periods. Additionally, our results also suggest shelf sediments are remobilized to make the turbidite deposits in SBB. Turbidities were characterized by a mixture of both lithogenic and biogenic sediment based on the elemental composition of the layers, a lower $\delta^{13}C$ (-22.57 ± 0.25‰), and a $\delta^{15}N$ (7.62 ± 0.21‰) that was indistinguishable from non-event (7.65 ± 0.24‰).

In contrast to flood sediments and turbidites, drought intervals were comprised of significantly higher $\delta^{15}N$ of 7.94 ± 0.09‰, while $\delta^{13}C$ signatures were similar to non-event events (-22.26 ± 0.02‰). This higher $\delta^{15}N$ may be a response to a combination of processes. The first is that a higher $\delta^{15}N$ could signal less terrestrial influence from reduced river discharge during drought conditions when rainfall was insufficient to produce river flow. However, the similarity of the $\delta^{13}C$ between drought and non-drought periods suggests that the OM is not terrestrial in origin and was influenced by marine processes instead. This second process relates to the introduction of warm, ETNP waters with high $\delta^{15}N$ into the region. During droughts, the North Pacific High strengthens and drives export productivity which in turn the expands the oxygen minimum zone (OMZ) in the ETNP (Wang et al., *this issue*). As the OMZ expands, water column denitrification increases as nitrate is utilized as a terminal electron acceptor and the $\delta^{15}N$ increases

(Altabet et al., 1995;. These ^{15}N rich waters then enter the SBB through the California Undercurrent and increase the $\delta^{15}N$ the phytoplankton uptake measured (Tems et al., 2016). A third process is also possible where droughts relate to with shifts to a negative PDO (cold phase) which also produces a shift in the source of surface water to the SBB (Tems et al., 2015). During a negative PDO, surface water in SBB is more influenced by the California Current, which also transports waters with a higher $\delta^{15}N$ value, this time from the Gulf of Alaska (Tems et al., 2015).

To better understand the sources of organic carbon, we utilized different chain length *n*-alkanes as biomarkers. The CPI ratio can be used to determine the freshness of carbon by exploiting the concept that *n*-alkanes with an odd number of carbon atoms are naturally produced (Eglinton and Hamilton 1967) whereas even chain *n*-alkanes are derived from petroleum or the alteration and production by bacteria. Our results suggested that non-event sediments are comprised of older, degraded material relative to flood sediments, even though the bulk C/N ratios are similar. The SBB is known to have a bacterial, *Beggiatoa* mat that sits overtop of the sediment and it is possible that the *Beggiatoa* mat can lower the CPI ratio (Grimalt et al, 1985; Nishimura et al., 1986; Elias et al., 1997). Additionally, there are abundant, naturally-occurring oil seeps in the SBB (Schimmelmann and Tegner, 1991) which can lower the CPI ratio as well as create a large unresolved complex mixture when run in the GC/MS (Blumer and Clark, 1967; Bray and Evans 1961). Therefore, the flood samples with larger CPI ratio ($p = 0.08$) had less bacterial degradation and petroleum influences relative to non-event samples. Drought and turbidite samples showed no even/odd differences relative to the non-event events.

To further constrain the source of sediment during floods, we utilized the distribution of odd chain *n*-alkanes and will focus specifically on flood, turbidite, and non-event sediment since drought *n*-alkane composition was not distinguishable from non-event *n*-alkane composition. Overall, terrestrial long chain (C_{27}, C_{29}, C_{31}) *n*-alkanes dominated the *n*-alkane composition in all of the sediments throughout the sediment core, similar to previous studies that focused on surface sediments (Bray and Evans, 1961; Crisp et al., 1979). Floods, however, were 4-fold higher (105 ± 47 compared to 27 ± 18 µg/gOC) in their concentrations of terrestrial *n*-alkanes compared to non-event sediment and turbidites were 2-fold higher in their concentrations of terrestrial *n*-alkanes compared to non-event sediment (46 ± 23 compared to 27 ± 18 µg/gOC) (Figure 3.3).

While terrestrial material is considered the dominant sediment source to the SBB, algal material still contributes to OC burial, especially during floods and turbidite remobilization. Floods and turbidite sediment had a 3-fold increase in marine algal *n*-alkanes (C_{15}, C_{17}, C_{19}) relative to non-event sediment (Table 3.4). The higher algal signal in turbidites was thought to come from the accumulation of biogenic sediment on the shelf before remobilization. During floods, the increased algal signal may be a result of increased riverine discharge carrying more nutrients into the SBB or storm-related mixing bringing more nutrients to the surface, stimulating phytoplankton growth. Previous work by Warrick et al. (2005) in the SBB, found that episodic rain events increase nutrient discharge into the basin. They found that algal biomass was highest in the surface waters of the basin rather than in the mouth of the Santa Clara River which suggests that our algal signal is majorly derived from marine algae rather than freshwater algae. A marine algal signal is further confirmed by our river end member samples

which, while they were not collected during a flood event, did not show any algal material present. Other studies have suggested that the greater source of nutrients to fuel phytoplankton growth is from upwelling (Warrick et al., 2005; Otero and Siegel, 2004). Weather patterns that increase precipitation in the region via atmospheric rivers are also accompanied by strong winds and storm conditions which have the potential to increase ocean mixing and introduce nutrients to the surface from deeper water (Waliser and Guan, 2017). Increased nutrients can then stimulate primary productivity and result in a greater burial of algal material in the basin.

Macrophyte *n*-alkanes (C_{21}, C_{23}) concentrations were significantly greater in flood sediments compared to non-event sediment (Figure 3.3). Macrophyte *n*-alkanes were about half that measured in the flood and most turbidite samples, and were completely absent during non-event periods. Previous studies in the SBB reported macrophyte *n*-alkanes in surface sediments, which suggests that our non-event samples were simply too dilute to detect macrophyte *n*-alkanes (Crisp et al., 1979). However, even with dilute samples, macrophyte *n*-alkanes were 4 times and 3 times higher in concentration for flood and turbidite sediments, respectively, compared to non-events (Table 3.4).

Macrophyte alkanes in the SBB most likely came from giant kelp, Macrocystis *pyrifera*, which is very abundant along the shoreline (Schimmelmann and Tegner, 1991). Kelp is a climate sensitive brown alga that dies with age, grazing, or by destruction by waves (Cavanaugh et al., 2011). Kelp is deposited on the ocean floor through two mechanisms that vary seasonally. In the summer, kelp accumulates on the kelp forest floor and then drifts to the basin center. In the winter, storms will destroy the kelp fronds

and form rafts that sink to the basin's floor (Schimmelmann and Tegner, 1991). It has been shown in recent years that severe storms and floods cause widespread destruction of kelp forests and substantially reduce their biomass (Schimmelmann and Tegner, 1991). We hypothesize that floods with storm conditions destroy kelp and transport their biomass into the deep basin. For flood years that did not have macrophyte *n*-alkanes, we hypothesized that the storm conditions during these periods may have been weaker, as low macrophyte concentrations correlate strongly with low algal concentrations (R^2 = 0.77), and act as indicators of ocean mixing or river discharge induced primary production.

While kelp is a contributor during flood events, its contribution to sediments is very little compared to the terrestrial contribution. This can be seen both by *n*-alkane composition as well by isotopic composition(Figure 3.1, Figure 3.2). Kelp measured had a higher $\delta^{13}C$ and $\delta^{15}N$ and compared to marine microalgal sources. These isotopic measurements of kelp are in agreement with previous studies showing kelp $\delta^{15}N$ to reflect $\delta^{15}N$ of surrounding water (Foley and Koch, 2010), and kelp to have a higher in $\delta^{13}C$ and $\delta^{15}N$ compared to the phytoplankton (Schimmelmann and Tegner, 1991; Page et al., 2008).

The magnitude and cause of floods in the SBB are not always the same. In order to link modern processes with those observed in the underlying sediments, we examined a major flood event that occurred in association with the 1997-1998 El Niño. The 1997-1998 El Niño was one of the wettest years on record and was reported to have an increase in lithogenic sedimentation rates from 1-2 g m^{-2} d^{-1} to 8 g m^{-2} d^{-1} (Lange et al., 2000).

However, while the 1998 flood was characterized by higher terrestrial *n*-alkane concentrations, it was significantly lower than that measured in the sediment core flood events. Combined, sediment trap terrestrial *n*-alkane flood concentrations were not significantly different from non-event sediment trap and sediment core measurements. Furthermore, no macrophyte material was detected in the 1997-1998 El Niño sediment trap samples despite there being records of kelp bed destruction during that time (Lange et al., 2000).

We suggest that the floods documented within the sediment core over the past 2000 years are megafloods- extreme floods brought about by very high quantities of precipitation. Megafloods are associated with atmospheric rivers that deposit massive amounts of precipitation relative to an El Niño event and can also be associated with storm conditions (Neiman et al., 2008; Dettinger et al., 2011). The most recent megaflood to occur in California was in 1861-1862 which coincides with the timing of the most recent flood event documented in the sediment core. The 1861-1862 megaflood, or "The Great Flood," occurred after ~ 40 days of continuous rain (Dettinger and Ingram, 2012). From our results these megfloods have the potential to bury significant quantities of organic carbon instantaneously. If we assume that all floods in our sediment core are megafloods, these events occur every 166 ± 48 years in SBB.

Overall, episodic events have a significant impact on carbon burial in the SBB. There were 11 megaflood events over the course of the past 2,000 years and they were responsible for burying 8% of the total OC buried in the sediment core. Of that OC, 82% consisted of a terrestrial carbon source. By sinking terrestrial organic carbon, it removes it from the terrestrial carbon cycle, where it had a greater chance of re-entering the

atmosphere by weathering. Megafloods also had the potential to bring storm conditions with it that not only destroyed kelp beds, but also increased algal material with increased mixing and nutrients in surface waters. On the other hand, of the 6 turbidites measured, they had remobilized OC so that it accounted for 10% of the total OC buried in the deep basin over the past 2,000 years. Of that OC, turbidites buried 14% of the total algal OC buried, 6% of the total macrophyte OC buried, and 7% of the total terrestrial OC buried in the deep basin. Thus, while non-event sediment is responsible for 82% of the total OC buried, the non-event sediments are only responsible for 69% of total algal OC buried, 72% of macrophyte OC buried, and 63% of terrestrial OC buried over the last 2,000 years.

CHAPTER 5

CONCLUSION

Floods events buried significant proportions of OC throughout geologic time. While these floods are rather rare, they are expected to occur every 150 years and have the potential to bury as much as 3% of the total OC buried throughout 2,000 years. The main source of OC buried during these episodic flood events is terrestrial, though algal and macrophytes are still contributors to the sediments. Increased algal concentrations are suspected to come from increased primary productivity due to increased nutrient load from river runoff and storm-driven mixing. Meanwhile, increased macrophytes are thought to come from the destruction kelp forests during flood associated storms. On the other hand, turbidites do not sequester new carbon to the sediments. Turbidite events are responsible for the instantaneous remobilization of sediment from the shelf to the deep basin. This OC can add up to 10% of the total OC buried in deep sea sediments over the past 2,000 years. Most of the turbidite OC is comprised of mix of biogenic and lithogenic sources. The impact of drought on OC sedimentation was very little, however, droughts were more influenced by denitrification in the ETNP or more influence from the California Current. Combined, our data indicated that non-event sedimentation was only responsible for 82% of the total OC buried.

REFERENCES

Altabet, M. A., Francois, R., Murray, D. W., & Prell, W. L. (1995). Climate-related variations in denitrification in the Arabian Sea from sediment 15N/14N ratios. *Nature, 373*(6514), 506-509. doi:10.1038/373506a0

Bao, H., Lee, T., Huang, J., Feng, X., Dai, M., & Kao, S. (2015). Importance of Oceanian small mountainous rivers (SMRs) in global land-to-ocean output of lignin and modern biospheric carbon. *Scientific Reports, 5*(1). doi:10.1038/srep16217

Barron, J. A., Bukry, D., & Field, D. (2010). Santa Barbara Basin diatom and silicoflagellate response to global climate anomalies during the past 2200 years. *Quaternary International, 215*(1-2), 34-44. doi:10.1016/j.quaint.2008.08.007

Barron, J. A., Bukry, D., & Hendy, I. L. (2015). High-resolution paleoclimatology of the Santa Barbara Basin during the Medieval Climate Anomaly and early Little Ice Age based on diatom and silicoflagellate assemblages in Kasten core SPR0901-02KC. *Quaternary International, 387*, 13-22. doi:10.1016/j.quaint.2014.04.020

Blair, N. E., Leithold, E. L., Ford, S. T., Peeler, K. A., Holmes, J. C., & Perkey, D. W. (2003). The persistence of memory: The fate of ancient sedimentary organic carbon in a modern sedimentary system. *Geochimica Et Cosmochimica Acta, 67*(1), 63-73. doi:10.1016/s0016-7037(02)01043-8

Blumer, M., & Clark Jr, R. C. (1967). DISTRIBUTION OF n-PARAFFINS IN MARINE ORGANISMS AND SEDIMENT. *Limnology and Oceanography, 12*(1), 79-87. doi:10.4319/lo.1967.12.1.0079

Bograd, S. J., Schwing, F. B., Castro, C. G., & Timothy, D. A. (2002). Bottom water renewal in the Santa Barbara Basin. *Journal of Geophysical Research: Oceans, 107*(C12). doi:10.1029/2001jc001291

Bond, G., Broecker, W., Johnsen, S., Mcmanus, J., Labeyrie, L., Jouzel, J., & Bonani, G. (1993). Correlations between climate records from North Atlantic sediments and Greenland ice. *Nature, 365*(6442), 143-147. doi:10.1038/365143a0

Brandes, J. A., Devol Allan, H., Yoshinari, T., Jayakumar, D. A., and Naqvi, S. W. A. (2003). Isotopic composition of nitrate in the central Arabian Sea and eastern tropical North Pacific: A tracer for mixing and nitrogen cycles. *Limnology and Oceanography, 43*(7),1680-1689.

Brassell, S. C., Eglinton, G., Marlowe, I. T., Pflaumann, U., & Sarnthein, M. (1986). Molecular stratigraphy: A new tool for climatic assessment. *Nature, 320*(6058), 129-133. doi:10.1038/320129a0

Bray, E., & Evans, E. (1961). Distribution of n-paraffins as a clue to recognition of source beds. *Geochimica Et Cosmochimica Acta, 22*(1), 2-15. doi:10.1016/0016-7037(61)90069-2

Burdige, D. J. (2006). *Geochemistry of marine sediments*. Princeton: Princeton University Press.

Cavanaugh, K., Siegel, D., Reed, D., & Dennison, P. (2011). Environmental controls of giant-kelp biomass in the Santa Barbara Channel, California. *Marine Ecology Progress Series, 429*, 1-17. doi:10.3354/meps09141

Cheung, S., Xia, X., Guo, C., & Liu, H. (2016). Diazotroph community structure in the deep oxygen minimum zone of the Costa Rica Dome. *Journal of Plankton Research, 38*(2), 380-391. doi:10.1093/plankt/fbw003

Crisp, P., Brenner, S., Venkatesan, M., Ruth, E., & Kaplan, I. (1979). Organic chemical characterization of sediment-trap particulates from San Nicolas, Santa Barbara, Santa Monica and San Pedro Basins, California. *Geochimica Et Cosmochimica Acta, 43*(11), 1791-1801. doi:10.1016/0016-7037(79)90027-9.

Dettinger, M. D., & Ingram, B. L. (2012). The Coming Megafloods. *Scientific American, 308*(1), 64-71. doi:10.1038/scientificamerican0113-64

Dettinger, M. D., Ralph, F. M., Das, T., Neiman, P. J., & Cayan, D. R. (2011). Atmospheric Rivers, Floods and the Water Resources of California. *Water, 3*(2), 445-478. doi:10.3390/w3020445

Deutsch, C., Berelson, W., Thunell, R., Weber, T., Tems, C., McManus, J., Crusius, J., Ito, T., Baumgartner, T., Ferreira, V., Mey, J., Geen, A. V. (2014). Centennial changes in North Pacific anoxia linked to tropical trade winds. *Science, 345*(6197), 665-668. doi:10.1126/science.1252332

Du, X., Hendy, I., & Schimmelmann, A. (2018). A 9000-year flood history for Southern California: A revised stratigraphy of varved sediments in Santa Barbara Basin. *Marine Geology, 397*, 29-42. doi:10.1016/j.margeo.2017.11.014

Eglinton, G., & Hamilton, R. J. (1967). Leaf Epicuticular Waxes. *Science, 156*(3780), 1322-1335. doi:10.1126/science.156.3780.1322

Elias, V. O., Simoneit, B. R., & Cardoso, J. N. (1997). Even *n*-Alkane Predominances on the Amazon Shelf and A Northeast Pacific Hydrothermal System. *Naturwissenschaften, 84*(9), 415-420. doi:10.1007/s001140050421

Emery, K., & Hülsemann, J. (1962). The relationships of sediments, life and water in a marine basin. *Deep Sea Research, 8*(3-4). doi:10.1016/0146-6313(61)90019-3

Emmer, E., & Thunell, R. C. (2000). Nitrogen isotope variations in Santa Barbara Basin sediments: Implications for denitrification in the eastern tropical North Pacific during the last 50,000 years. *Paleoceanography, 15*(4), 377-387. doi:10.1029/1999pa000417

Ficken, K., Li, B., Swain, D., & Eglinton, G. (2000). An *n*-alkane proxy for the sedimentary input of submerged/floating freshwater aquatic macrophytes. *Organic Geochemistry, 31*(7-8), 745-749. doi:10.1016/s0146-6380(00)00081-4

Foley, M., & Koch, P. (2010). Correlation between allochthonous subsidy input and isotopic variability in the giant kelp Macrocystis pyrifera in central California, USA. *Marine Ecology Progress Series, 409*, 41-50. doi:10.3354/meps08600

Goñi, M. A., Hatten, J. A., Wheatcroft, R. A., & Borgeld, J. C. (2013). Particulate organic matter export by two contrasting small mountainous rivers from the Pacific Northwest, U.S.A. *Journal of Geophysical Research: Biogeosciences, 118*(1), 112-134. doi:10.1002/jgrg.20024

Grimalt, J., Albaiges, J., Al-Saad, H. T., & Douabul, A. A. (1985). *n*-Alkane distributions in surface sediments from the Arabian Gulf. *Naturwissenschaften, 72*(1), 35-37. doi:10.1007/bf00405327

Hatten, J. A., Goñi, M. A., & Wheatcroft, R. A. (2010). Chemical characteristics of particulate organic matter from a small, mountainous river system in the Oregon Coast Range, USA. *Biogeochemistry, 107*(1-3), 43-66. doi:10.1007/s10533-010-9529-z

Hedges, J., Clark, W., Quay, P., Richey, J., Devol, A., Santos, U. de M. (1986). Compositions and fluxes of particulate organic material in the Amazon River. *Limnology and Oceanography, 31*(4), 717—738. doi:10.4319/lo.1986.31.4.0717

Hedges, J. I., & Keil, R. G. (1995). Sedimentary organic matter preservation: An assessment and speculative synthesis. *Marine Chemistry, 49*(2-3), 81-115. doi:10.1016/0304-4203(95)00008-f

Hendy, I. L., Dunn, L., Schimmelmann, A., & Pak, D. K. (2013). Resolving varve and radiocarbon chronology differences in the Santa Barbara basin sedimentary record, California. *Quaternary International, 387*, 155-168. doi:10.1016/j.quaint.2015.01.142

Hendy, I. L., Napier, T. J., & Schimmelmann, A. (2015). From extreme rainfall to drought: 250 years of annually resolved sediment deposition in Santa Barbara Basin, California. *Quaternary International, 387*, 3-12. doi:10.1016/j.quaint.2015.01.026

Hülsemann, J., & Emery, K. O. (1961). Stratification in Recent Sediments of Santa Barbara Basin as Controlled by Organisms and Water Character. *The Journal of Geology, 69*(3), 279-290. doi:10.1086/626742

Kennedy, J. A., & Brassell, S. C. (1992). Molecular records of twentieth-century El Niño events in laminated sediments from the Santa Barbara basin. *Nature, 357*(6373), 62-64. doi:10.1038/357062a0

Langbein, W. B., & Schumm, S. A. (1958). Yield of sediment in relation to mean annual precipitation. *Transactions, American Geophysical Union, 39*(6), 1076. doi:10.1029/tr039i006p01076

Lange, C. B., Weinheimer, A. L., Reid, F. M., Tappa, E., & Thunell, R. C. (2000). RESPONSE OF SILICEOUS MICROPLANKTON FROM THE SANTA BARBARA BASIN TO THE 1997-98 EL NINO EVENT. *California Cooperative Oceanic Fisheries Reports, 41*, 186-193.

Li, C., Sessions, A. L., Kinnaman, F. S., & Valentine, D. L. (2009). Hydrogen-isotopic variability in lipids from Santa Barbara Basin sediments. *Geochimica et Cosmochimica Acta, 73*(16).

Li, C., Sessions, A. L., Valentine, D. L., & Thiagarajan, N. (2011). D/H variation in terrestrial lipids from Santa Barbara Basin over the past 1400years: A preliminary assessment of paleoclimatic relevance. *Organic Geochemistry, 42*(1), 15-24. doi:10.1016/j.orggeochem.2010.09.011, 4803-4823.

Martin, J. H., Knauer, G. A., Karl, D. M., & Broenkow, W. W. (1987). VERTEX [Vertical Transport and Exchange]: Carbon cycling in the northeast Pacific. *Deep Sea Research Part B. Oceanographic Literature Review, 34*(9), 753. doi:10.1016/0198-0254(87)90148-8

Meyers, P. A. (1994). Preservation of elemental and isotopic source identification of sedimentary organic matter. *Chemical Geology, 114*(3-4), 289-302. doi:10.1016/0009-2541(94)90059-0

Meyers, P. A. (2003). Applications of organic geochemistry to paleolimnological reconstructions: a summary of examples from the Laurentian Great Lakes. *Organic Geochemistry, 34*(2), 261-289. doi:10.1016/s0146-6380(02)00168-7

Neiman, P. J., Ralph, F. M., Wick, G. A., Lundquist, J. D., & Dettinger, M. D. (2008). Meteorological Characteristics and Overland Precipitation Impacts of Atmospheric Rivers Affecting the West Coast of North America Based on Eight Years of SSM/I Satellite Observations. *Journal of Hydrometeorology*, *9*(1), 22-47. doi:10.1175/2007jhm855.1

Nishimura, M., & Baker, E. W. (1986). Possible origin of *n*-alkanes with a remarkable even-to-odd predominance in recent marine sediments. *Geochimica Et Cosmochimica Acta, 50*(2), 299-305. doi:10.1016/0016-7037(86)90178-x

Page H.M., Reed D.C., Brzezinski M.A., Melack J.M., Dugan J.E. (2008) Assessing the importance of land and marine sources of organic matter to kelp forest food webs. *Mar Ecol Prog Ser, 360,* 47–62.

Pearson, A., & Eglinton, T. (2000). The origin of n -alkanes in Santa Monica Basin surface sediment: A model based on compound-specific Δ 14 C and δ 13 C data. *Organic Geochemistry*, *31*(11), 1103-1116. doi:10.1016/s0146-6380(00)00121-2

Reimers, C. E., Lange, C. B., Tabak, M., & Bernhard, J. M. (1990). Seasonal spillover and varve formation in the Santa Barbara Basin, California. *Limnology and Oceanography, 35*(7), 1577-1585. doi:10.4319/lo.1990.35.7.1577

Scalan, E., & Smith, J. (1970). An improved measure of the odd-even predominance in the normal alkanes of sediment extracts and petroleum. *Geochimica Et Cosmochimica Acta, 34*(5), 611-620. doi:10.1016/0016-7037(70)90019-0

Schimmelmann, A., Lange, C. B., & Berger, W. H. (1990). Climatically controlled marker layers in Santa Barbara Basin sediments and fine-scale core-to-core correlation. *Limnology and Oceanography, 35*(1), 165-173. doi:10.4319/lo.1990.35.1.0165

Schimmelmann, A., Lange, C. B., & Meggers, B. J. (2003). Palaeoclimatic and archaeological evidence for a 200-yr recurrence of floods and droughts linking California, Mesoamerica and South America over the past 2000 years. *The Holocene*, 13(5), 763-778. doi:10.1191/0959683603hl661rp

Schimmelmann, A., & Tegner, M. J. (1991). Historical oceanographic events reflected in 13C/12C ratio of total organic carbon in laminated Santa Barbara Basin Sediment. *Global Biogeochemical Cycles, 5*(2), 173-188. doi:10.1029/91gb00382

Schimmelmann, A., Zhao, M., Harvey, C. C., & Lange, C. B. (1998). A Large California Flood and Correlative Global Climatic Events 400 Years Ago. *Quaternary Research, 49*(01), 51-61. doi:10.1006/qres.1997.1937

Sigman, D. M., Robinson, R., Knapp, A. N., Geen, A. V., Mccorkle, D. C., Brandes, J. A., & Thunell, R. C. (2003). Distinguishing between water column and sedimentary denitrification in the Santa Barbara Basin using the stable isotopes of nitrate. *Geochemistry, Geophysics, Geosystems, 4*(5). doi:10.1029/2002gc000384

Soutar, A., & Crill, P. A. (1977). Sedimentation and climatic patterns in the Santa Barbara Basin during the 19th and 20th centuries. *Geological Society of America Bulletin, 88*(8), 1161. doi:10.1130/0016-7606(1977)88<1161:sacpit>2.0.co;2

Soutar, A., Kling, S. A., Crill, P. A., Duffrin, E., & Bruland, K. W. (1977). Monitoring the marine environment through sedimentation. *Nature, 266*(5598), 136-139. doi:10.1038/266136a0

Sweeney, R. E., & Kaplan, I. (1980). Natural abundances of ^{15}N as a source indicator for near-shore marine sedimentary and dissolved nitrogen. *Marine Chemistry, 9*(2), 81-94. doi:10.1016/0304-4203(80)90062-6

Tems, C. E., Berelson, W. M., & Prokopenko, M. G. (2015). Particulate δ15N in laminated marine sediments as a proxy for mixing between the California Undercurrent and the California Current: A proof of concept. *Geophysical Research Letters, 42*(2), 419-427. doi:10.1002/2014gl061993

Tems, C. E., Berelson, W. M., Thunell, R., Tappa, E., Xu, X., Khider, D., Lund, S, Gonzalez-Yajimovich, O., & Hamann, Y. (2016). Decadal to centennial fluctuations in the intensity of the eastern tropical North Pacific oxygen minimum zone during the last 1200 years. *Paleoceanography, 31*(8), 1138-1151. doi:10.1002/2015pa002904

Thunell, R. C., Tappa, E., & Anderson, D. M. (1995). Sediment fluxes and varve formation in Santa Barbara Basin, offshore California. *Geology, 23*(12), 1083. doi:10.1130/0091-7613(1995)0232.3.co;2

Voss, M., Dippner, J. W., & Montoya, J. P. (2001). Nitrogen isotope patterns in the oxygen-deficient waters of the Eastern Tropical North Pacific Ocean. *Deep Sea Research Part I: Oceanographic Research Papers, 48* (8), 1905-1921.

Waliser, D., & Guan, B. (2017). Extreme winds and precipitation during landfall of atmospheric rivers. *Nature Geoscience, 10*(3), 179-183. doi:10.1038/ngeo2894